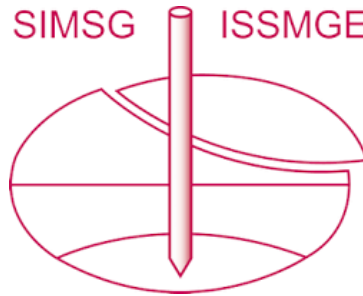


# INTERNATIONAL SOCIETY FOR SOIL MECHANICS AND GEOTECHNICAL ENGINEERING



*This paper was downloaded from the Online Library of the International Society for Soil Mechanics and Geotechnical Engineering (ISSMGE). The library is available here:*

<https://www.issmge.org/publications/online-library>

*This is an open-access database that archives thousands of papers published under the Auspices of the ISSMGE and maintained by the Innovation and Development Committee of ISSMGE.*

*The paper was published in the proceedings of the 20<sup>th</sup> International Conference on Soil Mechanics and Geotechnical Engineering and was edited by Mizanur Rahman and Mark Jaksa. The conference was held from May 1<sup>st</sup> to May 5<sup>th</sup> 2022 in Sydney, Australia.*

## Influences of unit cement content and fine fraction on freezing and thawing characteristics of soil pavement

Influences de la teneur en ciment et des fractions fines sur les caractéristiques de gel-dégel d'une chaussée sur sol

Takashi Kawamura & Takeo Umezaki

Department Civil Engineering and Water Environment, Faculty of Engineering, Shinshu University, Japan,  
t\_kawa@shinshu-u.ac.jp

**ABSTRACT:** Soil pavement, which is constructed by adding cement to soil, is flexible and offers a high water-retaining capacity. Its ability to ease the heat island phenomenon is expected. However, frost damage is a concern in snowy and cold regions. A series of tests of repeated freezing ( $-20\text{ }^{\circ}\text{C}$ ) and thawing ( $20\text{ }^{\circ}\text{C}$ ) was carried out for specimens with different unit cement contents and fine fraction. X-ray computerized tomography (CT) imaging was conducted during the test. Changes in specimen height and diameter were measured, and the generation of cracks in the specimen was investigated based on the CT images. The following results were obtained. In cases in which the fine fraction is larger than 30%, the freezing damage occurs remarkably. To prevent freezing damage to the soil pavement, the fine fraction is recommended to be smaller than 10% and the unit cement content is recommended to be larger than  $280\text{ kg/m}^3$ . By using CT images, it is possible to visualize the expansion deformation due to the freezing and generation of cracks in the specimen covered with ice in the freezing phase. It was suggested that the freezing and thawing characteristics could be evaluated quantitatively.

**RÉSUMÉ :** La chaussée sur sol, formée en ajoutant du ciment aux matériaux du sol, est souple et possède une grande capacité d'absorption d'eau. Elle réduit le phénomène d'îlot de chaleur. Toutefois, les dommages dus au gel sont à craindre dans les régions neigeuses et froides. Une série de tests de gel ( $-20\text{ }^{\circ}\text{C}$ ) et dégel ( $20\text{ }^{\circ}\text{C}$ ) répétés a été menée sur des échantillons à teneurs en ciment différentes et à fractions fines. Des images des échantillons aux rayons X et par tomographie assistée par ordinateur (TAO) ont été effectuées. Les mesures ont porté sur les modifications de hauteur et de diamètre des échantillons, et l'apparition de fissures dans les échantillons a été étudiée d'après l'imagerie aux rayons X et tomographique. Les résultats suivants ont été obtenus. Pour les cas où la teneur en fractions fines dépasse 30%, les dommages dus au gel sont visibles. Pour éviter la dégradation d'une chaussée sur sol par le gel, il est recommandé d'utiliser moins de 10% de fractions fines et une teneur en ciment de plus de  $280\text{ kg/m}^3$ . Grâce à la tomographie, il est possible de visualiser la déformation d'expansion due au gel et la création de fissures dans l'échantillon couvert de glace pendant la phase de gel. Cela suggère que les caractéristiques de gel et de dégel peuvent être évaluées quantitativement.

**KEYWORDS:** pavement, freezing and thawing, X-ray CT scanner

### 1 INTRODUCTION

Soil pavement, which is cement added to soil, has a high water-retaining capacity, and moderate flexibility and shock absorption. Therefore, it is expected to improve the heat island phenomenon and is applied to the park and sidewalk, as shown in Figure 1. However, its high water-retaining capacity makes frost damage, like frost heave and low-temperature cracks, a concern in snowy and cold region. Investigations of frost damage and the freeze-thaw resistance of soil pavement has not been performed sufficiently. Grain-sized distributions of soil influence the frost-heaving of ground. Kaplar (1974) reported on silt that contains soil particles sized less than  $0.02\text{ mm}$  with 30% or more frequency has a higher risk of frost heaving, as shown in Figure 2. On the other hand, soil cement formed by adding cement to soil material like the soil pavement. Unit cement content is one of the important parameters in designing the mixture for the soil cement.

In this paper, a series of repeated freezing and thawing was carried out to test specimens of soil pavement with different unit cement content and percentage by weight finer than  $0.02\text{ mm}$ . X-ray computer tomography (CT) imaging was carried out after every freezing and thawing phase. Based on the CT images, the deformation of the specimen and generation of cracks in the specimen, which cannot be measured directly during the freezing phase, were investigated, and changes in the height and diameter of the specimen were measured. The influences of unit cement

content and fine fraction on the freezing and thawing characteristics of soil pavement were investigated.

### 2 REPEATED FREEZING AND THAWING TEST

Saku soil, crushed stone, and Wakasato silt were used as soil materials. Grain-sized adjusted Saku soil, which is used in the practical construction works of soil pavement, was prepared by mixing Saku soil and crushed stone at a volume rate of 7 : 3. Its percentage by weight is finer than  $0.02\text{ mm}$ ,  $F_{002} = 7\%$ . Wakasato silt containing a high proportion of fine fraction was used to control fine fraction of the soil pavement specimen. Soil with a different percentage of samples finer than  $0.02\text{ mm}$  were prepared by mixing grain-sized adjusted Saku soil and Wakasato silt for a fixed rate. Grain-sized distribution curves of soil samples are shown in Figure 3.

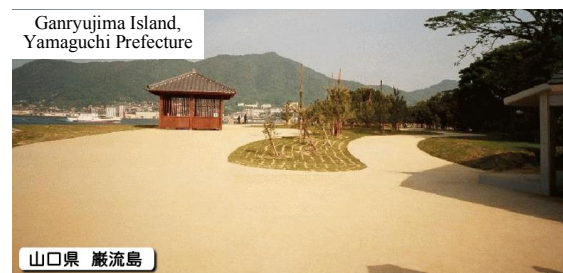


Figure 1. Example of soil pavement (SL KAGAKU Laboratory Corporation web page).

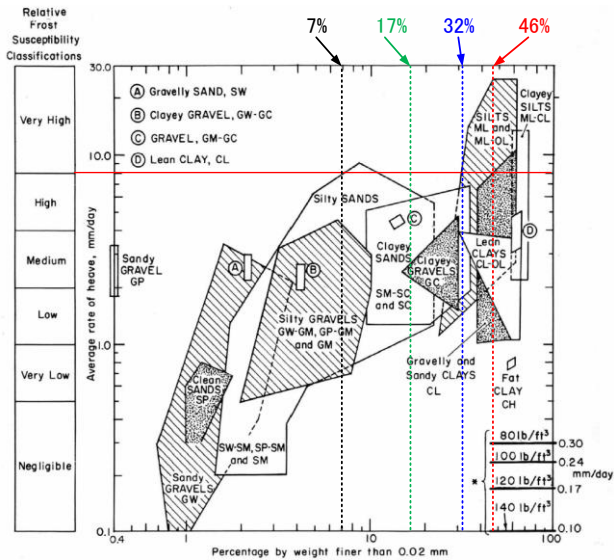


Figure 2. Estimation of frost heave based on particle size (modified from Kaplar, 1974).

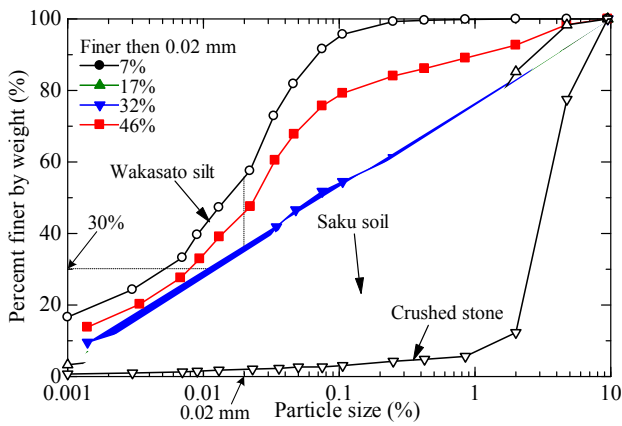


Figure 3. Particle size distribution.

Table 1. Test cases

(a) Test case 1: different unit cement content. The percentage by weight finer than 0.02 mm: 7%.

Finer than particle size 0.02 mm, $F_{0.02}$	Additive amount of cement for soil samples 100 L (kg)	Unit cement content, $C$ ( $\text{kg}/\text{m}^3$ )	Water-cement ratio, $W/C$
7%	50	457	41.2%
7%	25	276	75.7%
7%	12.5	144	151%

(b) Test case 2: different fine soil particle content. The additive amount of cement for soil samples 100 L: 50 kg.

Finer than particle size 0.02 mm, $F_{0.02}$	Additive amount of cement for soil samples 100 L (kg)	Unit cement content, $C$ ( $\text{kg}/\text{m}^3$ )	Water-cement ratio, $W/C$
7%	50	457	41.2%
17%	50	460	48.8%
32%	50	406	76.4%
46%	50	337	110%

Tables 1(a) and (b) show test cases. In test case 1 in Table 1(a), only the grain-sized adjusted Saku soil was used. The mass of cement added to 100 L of soil was set to 25 kg, which was used in practical construction. It also was set to twice and 0.5 times. The mass of cement added to soil corresponds with the unit cement content,  $C = 144 - 457 \text{ kg}/\text{m}^3$ . In test case 2 in Table 1(b),

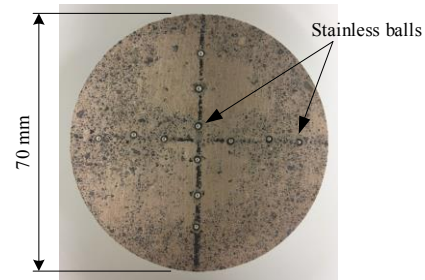


Figure 4. Targets on the top surface of the specimen.

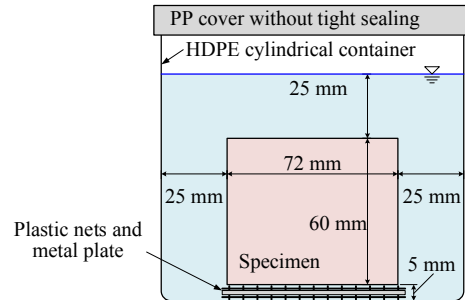


Figure 5. Specimen for the freezing and thawing test.

the mass of cement was fixed at twice the practical construction works and the mixing ratio of grain-sized adjusted Saku soil and Wakasato silt was set to 10 : 0, 8 : 2, 5 : 5 and 2 : 8. Percentages by weight finer than 0.02 mm were  $F_{0.02} = 7, 17, 32$  and 46%. Soil material in saturated surface dry condition is 18 kg (about 20 L), ordinary Portland cement is 5–1.25 kg, water is 1.8–5.5 L, the soil improvement agent (SL-1900 and SL-1900Z, SL KAGAKU Laboratory Corporation) is 0.54 L and pigment (iron oxide) was 0.08 kg. These components were mixed for 7 min and placed in a mold with 200 mm  $\times$  200 mm, 60-mm depth. Curing was performed in an indoor unit with a temperature of  $24 \pm 1 \text{ }^\circ\text{C}$  and humidity of  $80 \pm 5\%$ . The mold was released one day after the placement, and the samples were cured up to 28 days under the same conditions. A specimen with a 60-mm initial height and 72-mm initial diameter was prepared by core drilling. Twelve holes with diameters of 2.5 mm and depths of about 2.5 mm were drilled on the upper surface of the specimen, and 12 stainless balls with 2-mm diameters were placed there as a target, to measure the height of the specimen, as shown in Figure 4. As shown in Figure 5, the specimen was placed in a plastic container with a 110-mm inner diameter and was submerged in water for over 24 h, to absorb the water. To encourage freezing from the bottom of the specimen, the clearance with the bottom of the container was shortened, and a metal plate with high thermal conductivity was installed under the specimen.

Freezing and thawing were repeated in the submerged condition. The specimen was placed in a freezer at  $-20 \text{ }^\circ\text{C}$  for 24 h and in a constant temperature chamber at  $20 \text{ }^\circ\text{C}$  for 24 h or longer. The  $-20 \text{ }^\circ\text{C}$  of freezing and  $20 \text{ }^\circ\text{C}$  of thawing were repeated. The center of the specimen was frozen and thawed, as confirmed by another test using a specimen with a temperature sensor embedded inside, as shown in Figure 6. After every phase of freezing and thawing, X-ray CT imaging was performed using an X-ray CT scanner (Computed Tomography Equipment NAOMi-CT, RF Co., Ltd.) without taking the specimen out of the container. The height and diameter of the specimen were measured on two orthogonal vertical cross sections using NAOMi-CT Viewer Soft (RF Co., Ltd.) for CT images. The height was measured at the position where the stainless balls were installed, and the diameter was measured at heights of 10, 30 and 50 mm from the bottom of the specimen.

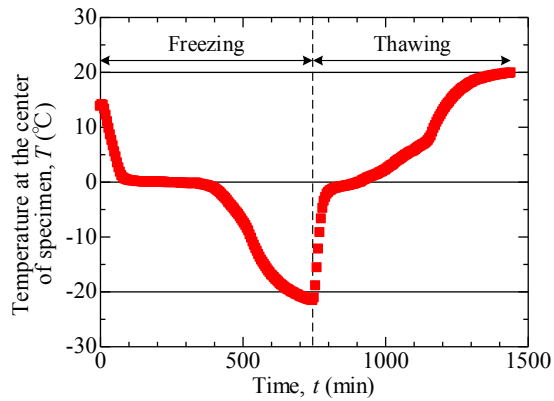


Figure 6. Example of the temperature at the center of the specimen in a freezing and thawing test.

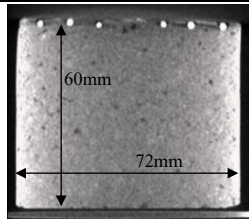
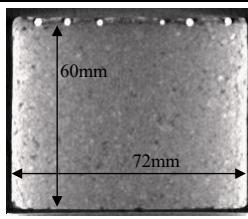
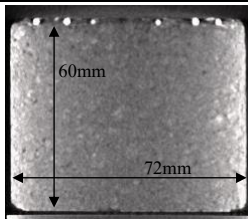
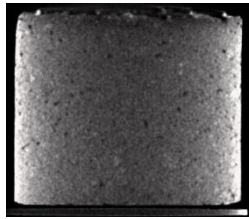
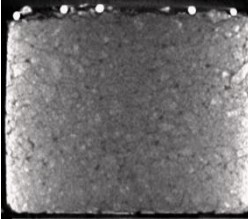
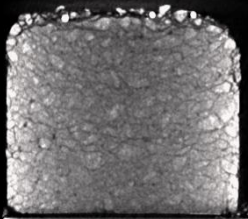
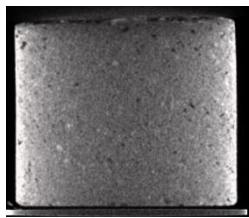
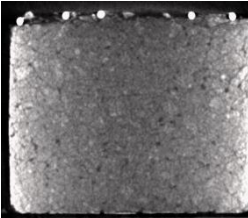
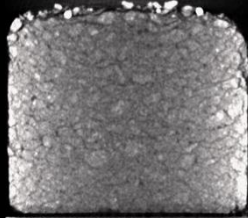
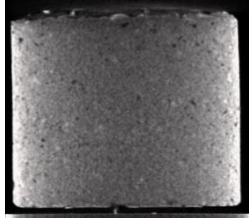
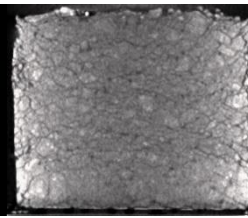
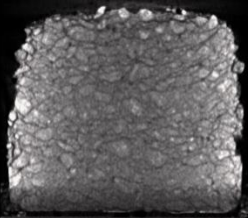
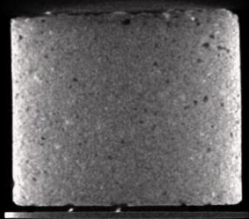
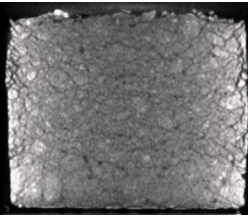
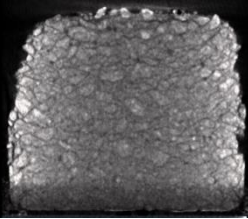
### 3 TEST RESULTS AND DISCUSSIONS

#### 3.1 Influence of unit cement content

Table 2 shows CT images of a vertical section of the specimen. Figures 7(a) and 7(b) show the change of axial strain,  $\varepsilon_a$ , and relationship of  $\varepsilon_a$  and radial strain,  $\varepsilon_r$ . The results for test case 1 with a different unit cement content,  $C = 457, 276$  and  $144 \text{ kg/m}^3$ , and the percentage by weight finer than  $0.02 \text{ mm}$ ,  $F_{0.02} = 7\%$ , are shown in Table 1(a). CT images with the same vertical section were extracted in each test, to the extent possible. The values of  $\varepsilon_a$  and  $\varepsilon_r$  are calculated from the average values of height and diameter at each measured values and the expansion is expressed positively.

As shown in Table 2, in the test case of  $C = 457 \text{ kg/m}^3$  of unit cement content, which is twice the amount of the practical construction works, no changes such as cracks inside the

Table 2. CT images after freezing and thawing for test case 1 with different unit cement content (percentage by weight finer than  $0.02 \text{ mm}$ :  $F_{0.02} = 7\%$ ).

	(a) $C = 457 \text{ kg/m}^3$	(b) $C = 276 \text{ kg/m}^3$	(c) $C = 144 \text{ kg/m}^3$
Initial condition			
	(a-1) $n = 0$	(b-1) $n = 0$	(c-1) $n = 0$
After freezing			
	(a-2) $n = 20, \varepsilon_a = 0.2\%$	(b-2) $n = 25, \varepsilon_a = 4.1\%$	(c-2) $n = 14, \varepsilon_a = 6.2\%$
After thawing			
	(a-3) $n = 20, \varepsilon_a = 0.5\%$	(b-3) $n = 25, \varepsilon_a = 3.9\%$	(c-3) $n = 14, \varepsilon_a = 4.7\%$
After freezing			
	(a-4) $n = 40, \varepsilon_a = 0.3\%$	(b-4) $n = 40, \varepsilon_a = 7.4\%$	(c-4) $n = 21, \varepsilon_a = 8.0\%$
After thawing			
	(a-5) $n = 40, \varepsilon_a = 0.2\%$	(b-5) $n = 40, \varepsilon_a = 6.2\%$	(c-5) $n = 21, \varepsilon_a = 5.7\%$

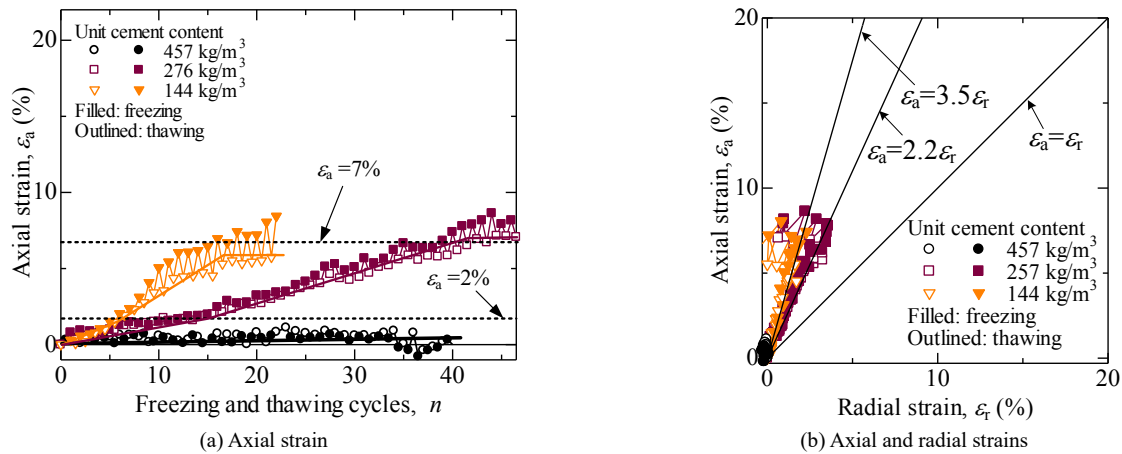


Figure 7. Test results for test case 1 with a different unit cement content (percentage by weight finer than 0.02 mm: 7%).

specimen are seen up to the freeze–thaw cycle,  $n = 40$ . The values of axial strain are lower than 1%, a significant increment not observed in Figure 7(a). When the soil material contains less than 10% soil particles finer than 0.02 mm and unit cement content is high, freezing damage hardly occurs. However, in the test cases of  $C = 144, 276 \text{ kg/m}^3$ , as the freeze–thaw cycle progresses, black streaks are seen inside the specimen and cracks are confirmed. The behavior that spreads cracks in the horizontal direction during the freezing phase and the cracks do not close completely during thawing is observed in CT images (Table 2). At the end of the test, cracks are distributed throughout the specimen. As shown in Figure 7(a), the axial strain gradually increases. Comparing the deformation in the freezing and thawing phases, the expansion deformation in the freezing phase is larger. The expansion deformation accumulates as the freeze–thaw cycle progresses, and the axial strain increases. In the test case of  $C = 144 \text{ kg/m}^3$ , which is about half the amount of the practical construction works, the amount of expansion deformation in one cycle significantly increases after  $n = 10$ . The behavior of the expansion deformation in the freezing phase and the shrinkage deformation in the immediately following thawing phase are clearly observed. In both cases of  $C = 144, 276 \text{ kg/m}^3$ , after the axial strain becomes larger than about 2%, the rate of increase in the axial strain becomes larger. When freezing and thawing are continued, the axial strain become  $\epsilon_a = 7\%$ , at  $n = 40$  in  $C = 276 \text{ kg/m}^3$ ,  $n = 14$  in  $C = 144 \text{ kg/m}^3$ . And after that, expansion and shrinkage are repeated without accumulating axial strain with freeze–thaw cycle, as shown in Figure 7(a). At this time, cracks spread over almost all the inside of the specimen, as shown in Table 2(b-4) and 2(c-4). New cracks developing is considered to be due to freezing decreases: freezing and thawing of pore water in the cracks is repeated and the specimen reaches the limit point at which the axial strain of the specimen does not increase any more. Scaling that part of the specimen is exfoliated at the surface, which can also be observed in the test cases of  $C = 144, 276 \text{ kg/m}^3$ . Especially at  $n = 40$  in the test case of  $C = 144 \text{ kg/m}^3$ , fragments of the specimen that fall off the side surface can be seen after thawing [Table 2(c-5)].

As shown in Figure 7(b), in the test cases of  $C = 144, 276 \text{ kg/m}^3$ , the relationship between axial and radial strains is almost linear. After the axial strain increases and the specimen reaches the limit, the scaling on the side of the specimen becomes remarkable, as shown in Table 2(b-5) and 2(c-5). The diameter of the specimen decreases, and it then seems that the radial strain decreases. The values of axial strain in the cases of  $C = 144, 276 \text{ kg/m}^3$  are approximately 2.2 to 3.5 times larger than those of the radial strain. The deformation behavior in the freezing–thawing test in this paper, in which the specimen is frozen from all surfaces, is different from the in-situ condition that the pavement is frozen in one direction from the top surface and the lateral

displacement hardly causes. However, in Saku City, Nagano Prefecture, Japan (normal value of the maximum and minimum temperatures from December to February is 4.2–7.4 °C, –7.5––4.7 °C), the freezing damage of the soil pavement with  $C = 276 \text{ kg/m}^3$  has not been observed. Under the tough conditions of repeating –20 °C freezing and 20 °C thawing in this paper, no visible cracks occur in the specimen up to  $n = 15$ . The axial strain of about 2% in the repeated freezing and thawing test can be considered to be an index to evaluate the frost damage of soil pavement.

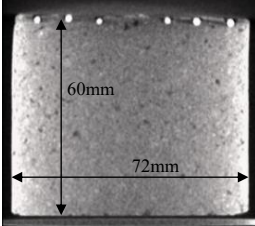
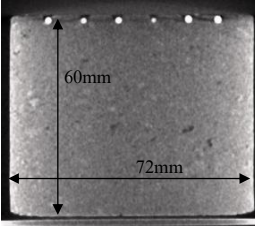
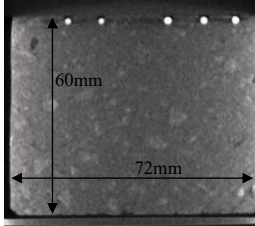
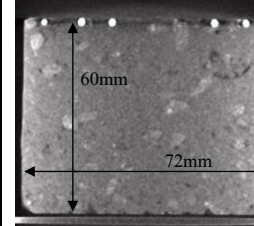
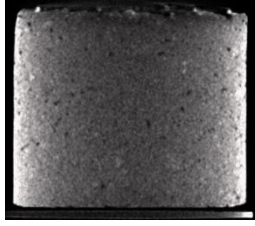
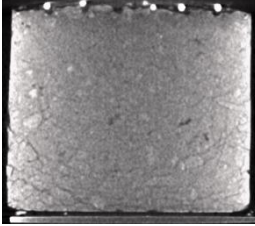
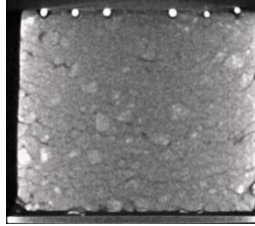
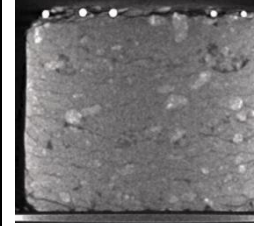
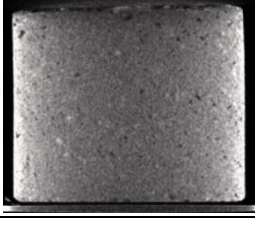
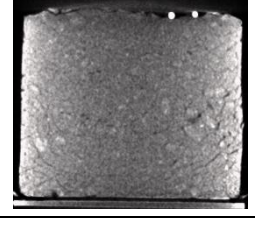
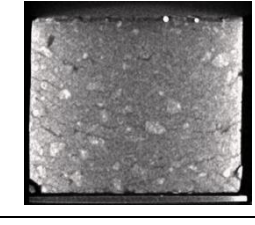
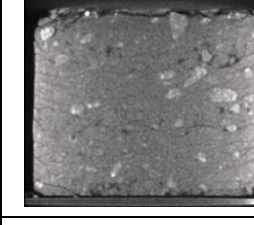
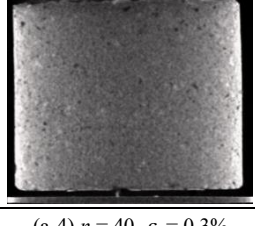
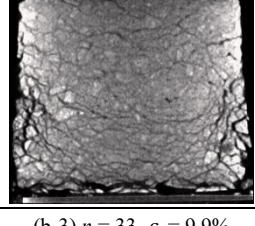
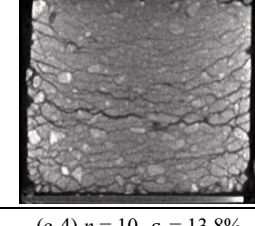
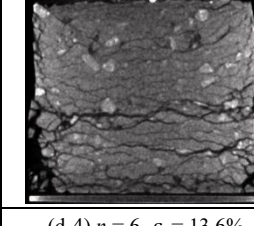
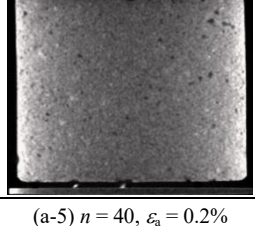
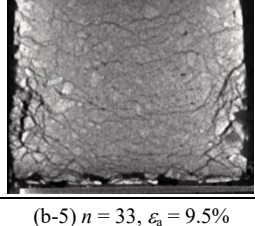
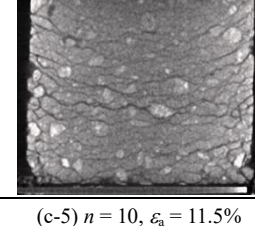
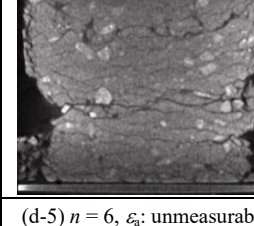
### 3.2 Influence of fine fractions

Table 3 and Figures 8(a) and 8(b) show CT images of a vertical section of the specimen, the change of  $\epsilon_a$ , and the relationship of  $\epsilon_a$  and  $\epsilon_r$  for the test case 2 shown in Table 1(b). The results for the test cases for the percentages by finer than 0.02 mm are  $F_{002} = 7, 17, 32$  and 46% and the constant additive amount of cement for soil samples 50 kg/100 L, which is twice the amount of the field works. In Table 3(a), the test case of  $F_{002} = 7\%$  is the same as the test case of  $C = 457 \text{ kg/m}^3$  in Table 2(a).

In the test cases of  $F_{002} = 17, 32$  and 46%, cracks occurred in the specimen after repeated freezing and thawing [Table 3(b), 3(c), and 3(d)], as well as the test cases of  $C = 144, 276 \text{ kg/m}^3$  shown in Table 2(b) and (c). At the end of the test, cracks are distributed over all of the specimen except of the upper part. As shown in Figure 8(a), the axial strain gradually increases as the freezing and thawing cycle increases. In the test cases of  $F_{002} = 32$  and 46%, the amount of deformation in one cycle is larger than that in the test cases shown in Figure 7(a) in which  $F_{002} = 7\%$  is constant and the unit cement content changes occur between  $C = 144, 276$  and  $457 \text{ kg/m}^3$ . The expansion deformation in the freezing phase and shrinkage deformation in the immediately following thawing phase are clear. The rate of increase in axial strain becomes larger after the strain becomes about 2%, similar to the behavior shown in Figure 7(a). After that, when the freezing and thawing are repeated, the axial strain reaches about 10%, which is larger than that in Figure 7(a), and the expansion and shrinkage are repeated without accumulating axial strain. The cycle in which the axial strain reaches about 10% is about  $n = 33$  at  $F_{002} = 17\%$  and  $n = 10$  at  $F_{002} = 32\%$ . In the test case of  $F_{002} = 46\%$ , the axial strain is about 14% after the freezing phase at  $n = 6$  [Figure 8(a)].

In addition, as shown in Table 3(c-4) and (d-4), the crack conditions are similar in the test cases of  $F_{002} = 32$  and 46%. In the test case of  $F_{002} = 46\%$ , which contains the largest amount of soil particles finer than 0.02 mm, the test was stopped because significant flaking occurred on the side of the specimen after the thawing phase of  $n = 6$ , shown in Table 3(d-5). However, if the freezing and thawing is repeated after  $n = 7$ , it is thought that the

Table 3. CT images during the freezing and thawing test for test case 2 with different fine particle content. The additive amount of cement for soil samples 100 L: 50 kg, which is twice amount of the field works.

	(a) $F_{002} = 7\% *$	(b) $F_{002} = 17\%$	(c) $F_{002} = 32\%$	(d) $F_{002} = 46\%$
Initial condition				
	(a-1) $n = 0$	(b-1) $n = 0$	(c-1) $n = 0$	(d-1) $n = 0$
After freezing				
	(a-2) $n = 20, \epsilon_a = 0.2\%$	(b-2) $n = 16, \epsilon_a = 3.8\%$	(c-2) $n = 4, \epsilon_a = 4.5\%$	(d-2) $n = 3, \epsilon_a = 4.8\%$
After thawing				
	(a-3) $n = 20, \epsilon_a = 0.5\%$	(b-3) $n = 16, \epsilon_a = 3.8\%$	(c-3) $n = 4, \epsilon_a = 4.5\%$	(d-3) $n = 3, \epsilon_a = 4.8\%$
After freezing				
	(a-4) $n = 40, \epsilon_a = 0.3\%$	(b-4) $n = 33, \epsilon_a = 9.9\%$	(c-4) $n = 10, \epsilon_a = 13.8\%$	(d-4) $n = 6, \epsilon_a = 13.6\%$
After thawing				
	(a-5) $n = 40, \epsilon_a = 0.2\%$	(b-5) $n = 33, \epsilon_a = 9.5\%$	(c-5) $n = 10, \epsilon_a = 11.5\%$	(d-5) $n = 6, \epsilon_a: \text{unmeasurable}$

\*: Same CT images as the test case of  $C = 457 \text{ kg/m}^3$  in Table 2(a).

expansion and shrinkage deformation is repeated without accumulating axial strain. In the test cases of  $F_{002} = 32$  and  $46\%$ , despite the unit cement content,  $C$ , is larger than practical construction works shown in Table 1(b). Freezing damage occurs in a small number of freezing and thawing cycle comparing the test case of  $F_{002} = 7\%$  and  $C = 276 \text{ kg/m}^3$  in Table 2(b), which is the same condition of the practical construction works. Even if the amount of unit cement content is doubled, if the percentages by finer than  $0.02 \text{ mm}$  is larger than  $30\%$ , the effect of freezing and thawing on the soil pavement will be large and freezing damage will be significant. Therefore, it is necessary to apply in snowy and cold region.

As shown in Figure 8(b), the relationships between axial and radial strains are generally linear, even when the percentages by

finer than  $0.02 \text{ mm}$  are large. In the test cases of  $F_{002} = 32\%$  and  $46\%$  in which the generation of cracks and accumulation of axial strain due to repeated freezing and thawing occur quickly, axial strain is much larger than radial strain, most likely because the specimen is restrained by the freezing of water around it and the generation of radial strain is disturbed.

#### 4 CONCLUSIONS

A series of repeated freezing and thawing test was carried out for specimens with different unit cement content and a percentage by weight finer than  $0.02 \text{ mm}$ . X-ray CT imaging was carried out after every freezing and thawing phase, and changes in the height

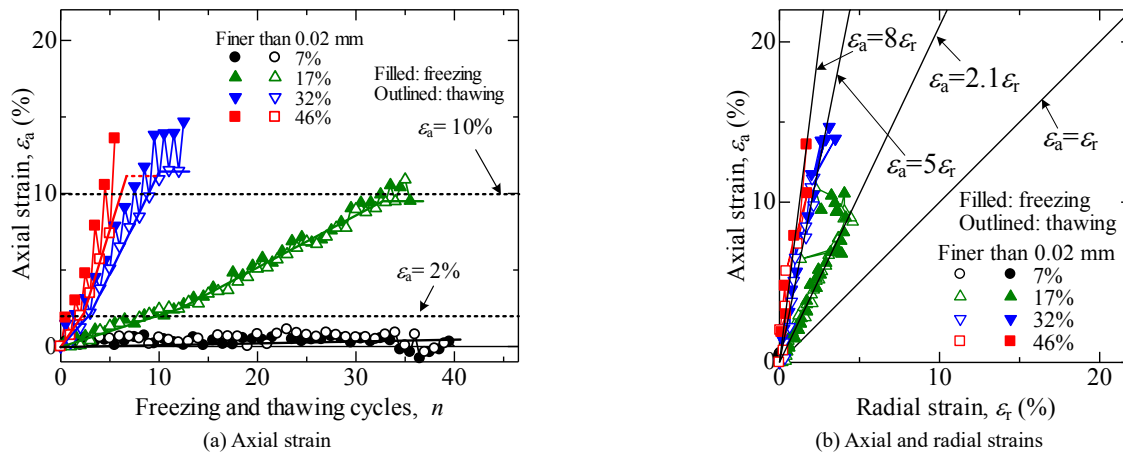


Figure 8. Test results for test case 2 with different fine particle content. The additive amount of cement for soil samples 100 L: 50 kg.

and diameter of the specimen were measured based on X-ray CT images. The influences of cement content and fine fraction on the freezing and thawing characteristics of soil pavement were investigated. The main conclusions are as follows.

- 1) In both cases, with different unit cement content and fine fraction, when the axial strain during freezing and thawing becomes larger than about 2%, cracks are generated inside the soil pavement specimen.
- 2) When freezing and thawing is repeated further, axial strain increases to 7–10%, and then the strain hardly increases where new crack generation subsides and freezing and thawing of water in the crack are repeated.
- 3) In the cases in which the percentage by weight finer than 0.02 mm is larger than 30%, the freezing damage occurs remarkably.
- 4) To prevent freezing damage of soil pavement, it is recommended that the percentage by weight finer than 0.02 mm is smaller than 10% and the unit cement content is larger than 280 kg/m<sup>3</sup>.
- 5) By using CT images, it is possible to visualize the expansion deformation due to freezing and generation of cracks in the specimen covered with ice in the freezing phase. It was suggested that the freeze–thaw characteristics could be evaluated quantitatively.

## 5 ACKNOWLEDGEMENTS

This work was supported by JSPS KAKENHI Grant Number 18K04300. Saku soil, crushed stone, and soil improvement agent were provided from Hirabayashi Co., Ltd. The X-ray CT scanner system (Computed Tomography Equipment NAOMi-CT) and the image analysis software (NAOMi-CT Viewer Soft) were donated by RF Co., Ltd.. The experiment was carried out as part of graduation research of Mr. Yuki Fukuda and Ryo Kajiyama, formerly of Shinshu University. The authors are deeply grateful to them.

## 6 REFERENCES

- Kaplar, C. W.: Freezing Test for Evaluating Relative Frost Susceptibility of Various Soils, DTIC Document, 1974.
- SL KAGAKU Laboratory Corporation web page < <http://www.sl-kagaku.com/> > (in Japanese, access date: 11/11/2020).